Geology, Geophysics & Environment 2026, vol. 52 (1): 87–102

Application of seismic refraction methods for rock mass characterization at the lead mine tailings site in Olovo Mine

Ekrem Bektašević[1], Krzysztof Skrzypkowski[2], Semir Kahrimanović[3], Luka Crnogorac[4], Kemal Gutić[5]

[1] *University of Tuzla, Faculty of Mining, Geology and Civil Engineering, Tuzla, Bosnia and Herzegovina, e-mail: ekrem.bektasevic@untz.ba, ORCID ID: 0000-0001-6742-966X*
[2] *AGH University of Krakow, Faculty of Civil Engineering and Resource Management, Krakow, Poland, e-mail: skrzypko@agh.edu.pl (corresponding author), ORCID ID: 0000-0003-0819-2345*
[3] *GEOMET Ltd., Olovo, Bosnia and Herzegovina, e-mail: semir.kahrimanovic@geomet.ba*
[4] *University of Belgrade, Faculty of Mining and Geology, Belgrade, Serbia, e-mail: luka.crnogorac@rgf.bg.ac.rs, ORCID ID: 0000-0002-9897-270X*
[5] *University of Tuzla, Faculty of Mining, Geology and Civil Engineering, Tuzla, Bosnia and Herzegovina, e-mail: kemal.gutic@untz.ba, ORCID ID: 0009-0008-9107-4641*

Received: 12 February 2026; accepted: 2 April, 2026; first published online: 30 April, 2026

Abstract: In this study, the application of seismic refraction for the characterization of the rock mass at the lead mine tailings facility in Olovo is presented, with the aim of identifying lithostratigraphic horizons, structural discontinuities, and zones of reduced mechanical resistance that may affect tailings stability. The investigations were conducted along seven seismic profiles of varying lengths and resolutions, designed to cover both shallow and deeper portions of the rock mass to a depth of approximately 60 m. Data processing and interpretation were carried out using the Delta-t-V seismic tomography method, which enables reliable reconstruction of P-wave velocities even under conditions of complex geological structure and velocity inversions. The obtained results indicate pronounced heterogeneity of the rock mass, with clearly differentiated zones of surface embankments and unconsolidated materials (600–1,200 m/s), transitional zones of degraded and karstified rocks (1,800–3,200 m/s), and basal horizons of compact limestone, where P-wave velocities reach values of approximately 4,400 m/s. Particular attention was given to locally developed low-velocity anomalies within deeper horizons, interpreted as karst structures and cavernous zones that are potentially critical for tailings stability. By integrating the individual profiles, a unified 3D rock mass model was developed, enabling spatial analysis of anomalies and reliable terrain zoning. The results confirm that seismic refraction, combined with the Delta-t-V method, represents an efficient, non-destructive, and engineering-relevant tool for characterizing complex tailings rock masses. The developed models have direct application in stability assessment, remediation planning, and the enhancement of mining and environmental safety systems.

Keywords: non-destructive methods, applied geophysics, seismic tomography, P-wave velocities

INTRODUCTION

Geophysical investigations represent an indispensable component of modern mining engineering and geotechnical practice, as they enable the non-destructive characterization of subsurface structures and rock masses (Bektašević et al. 2025a, 2025b, 2025c). Their application in mining projects offers multiple advantages, including cost reduction, environmental preservation, and improved infrastructure safety (Ackman & Cohen 1994, Adewoyin et al. 2021a). Unlike invasive methods such as drilling and excavation, geophysical techniques provide continuous information about subsurface layers, thereby facilitating an integrated understanding of geological conditions (Cheng et al. 2025, Akinlalu et al. 2026). Among geophysical techniques, seismic refraction occupies a prominent position. It is based on measuring the travel times of elastic waves through different lithological layers, enabling precise identification of lithostratigraphic horizons, P-wave velocities, and structural discontinuities (Akinlalu et al. 2026). The seismic refraction method is widely applied in engineering geology, hydrogeology, civil engineering, and mining engineering (Yilmaz 2001, Hill 2025). Its non-destructive nature makes it particularly suitable for investigations of tailings facilities, where additional interventions in already stressed environments must be minimized (Mollehuara-Canales et al. 2021).

The lead mine in Olovo, located in the central part of Bosnia and Herzegovina, has a long tradition of mineral resource exploitation. Over decades of mining activity, significant quantities of tailings have been generated and deposited in tailings storage facilities. Tailings facilities represent complex engineering structures whose stability depends on the geological and geotechnical characteristics of the foundation (Lottermoser 2010). Their safety is of technical, environmental, and social importance: technically, due to the preservation of mining infrastructure; environmentally, because of potential impacts on groundwater and surface water systems; and socially, as it directly affects the health and safety of the local population (Vick 1990, U.S. EPA 2026). Geophysical investigations of the Olovo lead mine tailings facility have dual significance. On the one hand, they contribute to the safety of mining operations, and on the other, they ensure environmental protection and safeguard the local community (Idziak & Dubiel 2011). The application of seismic refraction in this context makes it possible to identify subsurface layers to depths ranging from 20 to 60 m, including fractures, cavities, and other anomalies that may influence structural stability (Cardarelli et al. 2010, Akingboye & Ogunyele 2019). The particular value of this research lies in the application of the Delta-t-V method, which enables continuous tomographic interpretation of P-wave velocities. In contrast to classical refraction methods, which were limited by the occurrence of velocity inversions, the Delta-t-V approach makes reliable interpretation under complex geological conditions possible, including karstified limestones, degraded rock masses, and heterogeneous alluvial sediments (Herlambang & Riyanto 2021, Wang H. et al. 2025). This significantly expands the applicability of seismic refraction in addressing complex geological problems (Hanafi et al. 2025).

Previous studies have demonstrated the broad application of seismic refraction in mining engineering, civil engineering, and hydrogeology. Examples from Europe highlight its use in terrain zoning, tunnel design, identification of unstable zones, and landslide risk assessment (Tajudin et al. 2016). In the mining sector, it has proven to be an effective tool for planning drilling campaigns, sampling programs, and the design of mine waste repositories (Adewoyin et al. 2021b). Environmental applications include groundwater contamination risk assessment and the identification of zones of increased porosity that may serve as pathways for pollutant migration (Akingboye 2025). The scientific contribution of this study lies in demonstrating how seismic refraction, combined with the Delta-t-V method, can provide a reliable characterization of the rock mass beneath a tailings facility. The obtained results enable precise identification of lithostratigraphic horizons, P-wave velocities, and structural discontinuities, thereby establishing a foundation for safer design and improved sustainability of mining facilities (Pegah & Liu 2016, Bačić et al. 2020, Fisseha et al. 2021). In this way, the study bridges the theoretical foundations of seismic methods with the practical challenges of mining engineering and

environmental protection, emphasizing the importance of an integrated approach in tailings investigations (Watts et al. 2022, Allen et al. 2025).

MATERIALS AND METHODS

Due to these geological specificities, seismic refraction was selected as the most appropriate method, as it enables the identification of lithostratigraphic horizons and discontinuities within the rock mass. In this study, seismic refraction was applied as the primary method for detailed characterization of the rock mass underlying the tailings facility. The methodological approach was based on the design of seven seismic profiles (RFP-1 to RFP-7), whose spatial distribution provided comprehensive insight into lithological horizons and structural anomalies. Particular attention was given to the configuration of the geophone array and the selection of shot points in order to achieve optimal data resolution and reliable interpretation of layers with varying degrees of consolidation. Data processing was carried out using the Delta-t-V method, which proved suitable for the complex geological conditions of the tailings facility. Its application enabled continuous tomographic reconstruction of P-wave velocities, allowing precise identification of velocity gradients and inverse velocity distributions commonly observed in karstified limestones and degraded rock masses. In this way, the adopted methodology ensured that the heterogeneous rock mass was interpreted as an integrated system, minimizing the risk of misclassification of lithological horizons (Cai et al. 2014, Xie et al. 2024, Jian et al. 2025). In addition to the Delta-t-V method, other tomographic algorithms are widely applied in engineering geophysics, such as SIRT (Simultaneous Iterative Reconstruction Technique) and Fast Shortest Path Ray Tracing. The SIRT method enables iterative reconstruction of velocity models with control over solution smoothness, while the Fast Shortest Path algorithm efficiently computes ray paths through heterogeneous models and provides stable results in complex geological conditions. Compared to these, the Delta-t-V approach has proven suitable for interpreting inverse velocity sequences and vertical gradients, particularly in the karstified limestones and degraded zones characteristic of the study area. Nevertheless, it should be emphasized that Delta-t-V is used as a complement to standard algorithms rather than as their replacement.

Geophysical investigations were carried out within Zone 4 of the tailings facility of the lead mine in Očekalj, located within the exploitation field of the Olovo mine. The geological context of the investigated area is characterized by a complex lithological structure, marked by the presence of karstified limestones, degraded rock masses, and heterogeneous alluvial sediments. Such a combination of lithological units creates a heterogeneous rock mass with significant variations in consolidation and porosity, requiring the application of methods capable of reliably detecting and interpreting layers with differing mechanical properties (Maniscalco et al. 2022). The study area belongs to the broader geological framework of the Dinaric Alps, dominated by Mesozoic carbonate rocks that are highly susceptible to karstification and tectonic fracturing. Regional tectonic lineaments trending northwest–southeast have conditioned the formation of degraded zones and occasional cavities within the limestone mass. These specificities strongly influence seismic wave propagation and the interpretation of velocity anomalies. To provide a broader geographic context, the study area is located within the Olovo lead mine in northeastern Bosnia and Herzegovina (approximate coordinates: 44°05′58.68″N, 18°37′13.45″E). The geophysical survey was conducted in Zone 4 of the tailings facility. The layout of the geophysical survey, including the clearly marked positions of the refraction profiles, is shown in Figure 1.

Seven refraction seismic profiles (RFP-1 to RFP-7) were designed to cover representative portions of the rock mass. Profile lengths and geophone spacing were defined through optimization between the required resolution and actual field conditions, rather than arbitrarily selected. The longer profiles (RFP-1 to RFP-3) made it possible to investigate the deeper lithostratigraphic horizons to depths of approximately 60 m, whereas the shorter profiles (RFP-4 to RFP-7) were focused on detailed characterization of shallower structures down to approximately 40 m. This design concept ensured a balanced relationship between horizontal and vertical resolution, which is essential for reliable interpretation of a heterogeneous rock mass (Wei & Fu 2014, Kalashnikova et al. 2020, Musmann 2023, Sun et al. 2025, Wang H. et al. 2025).

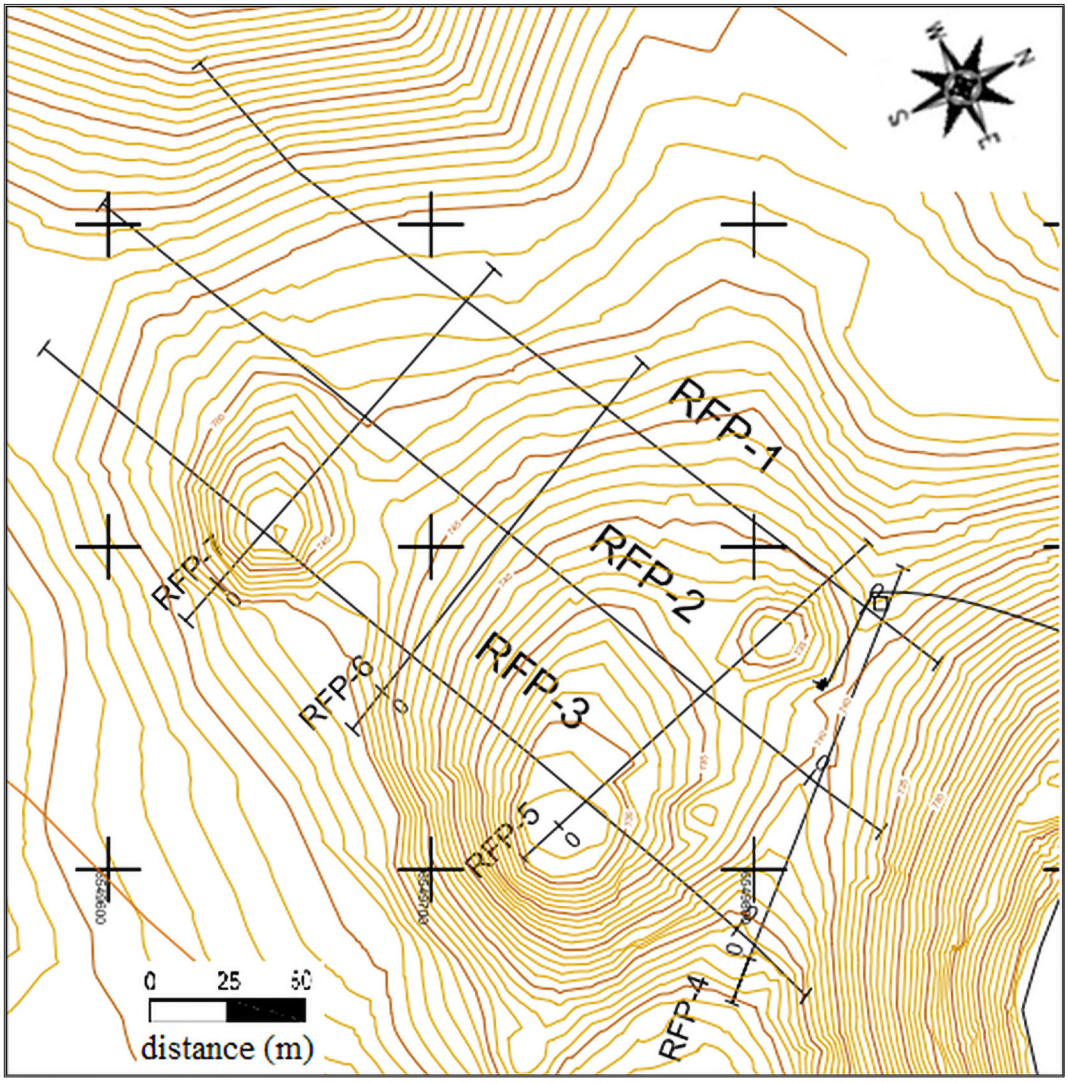

Fig. 1. *Layout of the geophysical survey showing the positions of the refraction profiles (RFP-1 to RFP-7) within Zone 4 of the lead mine tailings facility in Olovo (CTU IPKIN 2022)*

For clarity in presenting the field implementation of the designed profiles, the basic technical parameters of the refraction seismic measurements and schematic layouts for two profile groups are provided below. The profiles were differentiated according to their length, geophone spacing, and expected depth of investigation, thereby adapting the methodology to the local geological conditions and research objectives. A geophone spread length of 230 m was applied, with a total investigation length of 290 m, for profiles RFP-1, RFP-2, and RFP-3. Measurements were conducted using 24 seismic channels per record and 11 shot points evenly distributed along the profile, ensuring stable registration of first arrivals and reliable tomographic reconstruction of P-wave velocities. The geophone spacing was 10 m, resulting in an effective depth of investigation of approximately 60 m. A schematic layout of the spread configuration and measurement parameters for this group of profiles is shown in Figure 2.

Profiles RFP-4 to RFP-7 were designed with a shorter geophone spread length of 115 m and a total investigation length of 145 m. In this case as well, a 24-channel seismic system with 11 shot points per profile was employed, while the geophone spacing was reduced to 5 m in order to increase the resolution within the near-surface and sub-surface layers.

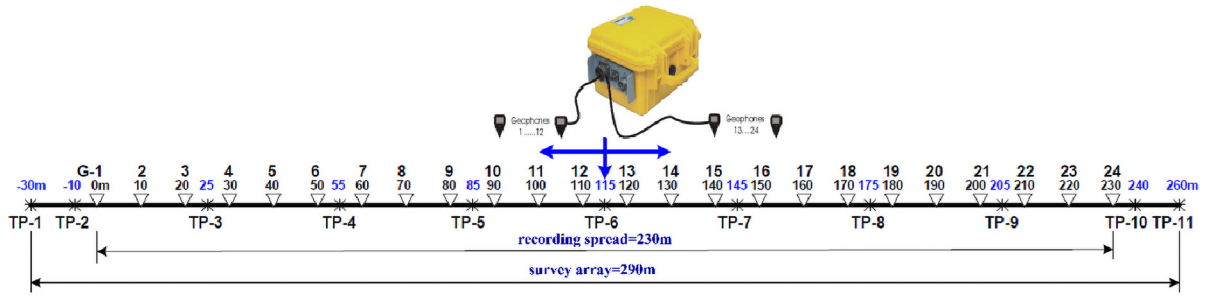

Fig. 2. *Schematic layout of the field acquisition parameters for refraction seismic profiles RFP-1 to RFP-3. The figure illustrates the positions of 24 seismic channels with a 10 m geophone spacing (total spread length of 230 m) and 11 shot points (TP – test point) distributed at the beginning, end, and along the profile. This configuration provides multi-fold coverage and an effective investigation depth of up to 60 m (CTU IPKIN 2022)*

The reduction of the geophone spacing to 5 m for profiles RFP-4 to RFP-7 directly resulted in a decrease in the radius of the first Fresnel zone, thereby achieving the superior lateral resolution necessary for detecting smaller karst voids and fracture zones within the surface layer. Although the Fresnel zone concept is traditionally associated with seismic reflection, in refraction tomography, it defines the "volume of sensitivity" (sensitivity kernels) around the ray path. The horizontal resolution is intrinsically linked to the width of the first Fresnel zone; features smaller than this zone are difficult to resolve as the recorded signal represents an average of the physical properties within that volume.

By reducing the geophone spacing from 10 m (RFP-1 to RFP-3) to 5 m (RFP-4 to RFP-7), the width of the first Fresnel zone was significantly narrowed, directly enhancing the lateral resolution. For the 10 m spacing, the theoretical horizontal resolution is approximately 10–20 m, whereas for the 5 m spacing, it improves to 5–10 m. This configuration makes it possible to reliably detect lateral discontinuities and karst features (e.g., voids or fracture zones) with horizontal dimensions exceeding 5 m. The vertical resolution, defined as a quarter of the wavelength (λ/4), is estimated at approximately 3–5 m in the near-surface layers, depending on the dominant source frequency and local velocities.

The applied variation in profile geometry enabled an optimal balance between regional structural mapping of deeper horizons and high-resolution detection of local anomalies. This configuration enabled reliable investigation of the rock mass to depths of approximately 40 m, in accordance with the objectives of detailed characterization of degraded and engineering-sensitive zones. The corresponding schematic layout of the spread configuration is presented in Figure 3.

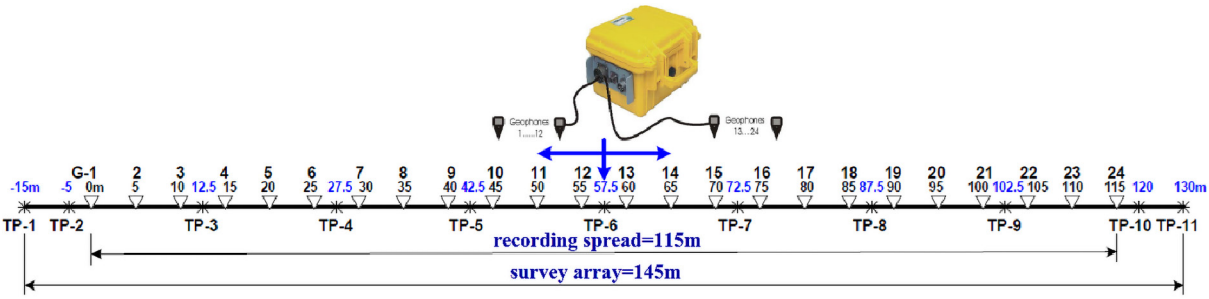

Fig. 3. *Schematic layout of the field acquisition parameters for refraction seismic profiles RFP4–7. The figure illustrates a high-resolution configuration utilizing 24 channels with a reduced geophone spacing of 5 m (total spread length of 115 m). With 11 shot points (TP – test point) per profile, this setup increases the ray-path density in the near-surface zone, providing superior lateral resolution for the detection of localized karst features to a depth of approximately 40 m (CTU IPKIN 2022)*

Seismic measurements were carried out using modern geophysical equipment selected in accordance with the research objectives and specific field conditions. A *Geometrics Geode* 24-channel digital seismograph was employed, which is widely reported in the literature as a reliable instrument for near-surface investigations due to its high accuracy in recording first P-wave arrivals (Steeples 2005, Adewoyin et al. 2021c, Kuehn 2024). Geo Space geophones with a natural frequency of 4 Hz were deployed along the profiles in accordance with the designed spread configuration, ensuring optimal sensitivity and minimal signal distortion (Dean & Grant 2024). The seismic source consisted of an 8 kg sledgehammer in combination with a steel base plate, representing standard practice in near-surface seismology and engineering geology (Sheriff & Geldart 1995, Yilmaz 2001, Brom & Stan Kleczek 2015, Pegah & Liu 2016, Foti et al. 2018). This source configuration generations elastic waves with sufficient energy to achieve investigation depths of up to 60 m, while minimizing disturbances and eliminating the need for explosive materials. Consequently, the methodology retained its non-destructive character, which is particularly important in tailings investigations where additional structural disturbance must be avoided. Special attention was devoted to real-time visual quality control of shot records. At each source location, vertical stacking of a minimum of 5 to 10 hammer blows was performed, significantly improving the signal-to-noise (S/N) ratio. This procedure effectively reduced the noise generated by surrounding mining machinery, enabling precise manual picking of first P-wave arrivals even at the most distant geophones. The main acquisition parameters of the refraction seismic surveys are presented in Table 1.

The combination of a high-precision seismograph, low-frequency geophones, and an impact seismic source ensured the acquisition of clear and reliable signals. This provided a high-quality dataset for subsequent processing using the Delta-t-V method, thereby ensuring the scientific validity and practical applicability of the research results.

Table 1
Main acquisition parameters of refraction seismic surveys

Parameter	RFP-1 to RFP-3	RFP-4 to RFP-7
Seismograph	Geometrics Geode (24-channel)	Geometrics Geode (24-channel)
Number of channels per record	24	24
Geophone type	Geo Space	Geo Space
Geophone natural frequency	4 Hz	4 Hz
Geophone spacing	10 m	5 m
Geophone spread length	230 m	115 m
Total investigation length	290 m	145 m
Number of shot points	11	11
Seismic source	8 kg sledgehammer + steel plate	8 kg sledgehammer + steel plate
Stacking per shot point	5–10 hammer blows	5–10 hammer blows
Approximate depth of investigation	60 m	40 m

DELTA-T-V METHOD

A total of 77 shot records (11 shot points per profile) were processed for the seven seismic refraction lines. P-wave travel times (first-breaks) were determined using manual picking within the software environment. Each seismogram was visually inspected to identify signal arrivals across all source-geophone offsets. This procedure was conducted to account for the specific ambient noise conditions of the site. The Delta-t-V method was introduced into practice in the late 1990s, with its theoretical foundation provided by Gebrande and Miller (1985). Its principal advantage lies in enabling a continuous velocity distribution with depth beneath each geophone location, including vertical velocity gradients, linear velocity increase with depth, and inverse velocity structures. The method is based on

transforming the travel times into a depth profile, where the depth to the refractor (z) is approximated using the delay-time concept according to the relation (Gebrande & Miller 1985):

$$z = \frac{\Delta t \cdot V_1 \cdot V_2}{\sqrt{V_2^2 - V_1^2}} \quad (1)$$

where Δt represents the time difference obtained from the intersection of travel-time curves corresponding to opposite shooting directions.

In this way, the limitation of classical refraction methods requiring a "normal velocity sequence" ($V_2 > V_1$) is overcome. The Delta-t-V method has proven particularly useful in karstified limestones and degraded rock masses, such as those present in the investigated area (Sheehan et al. 2005, Bačić et al. 2020, Padovan et al. 2025). Numerical processing and tomographic inversion of the data were performed using the ReflexW software package (Sandmeier 2016). The Delta-t-V method was applied to generate the initial 1D/2D velocity model, which served as the starting distribution for the final tomographic optimization. The final inversion was conducted using the SIRT (Simultaneous Iterative Reconstruction Technique) algorithm over 20 iterations, incorporating smoothing algorithms to eliminate numerical artifacts. The quality and reliability of the tomographic inversion were validated through statistical analysis of deviations between observed and calculated P-wave travel times using the root mean square error (RMSE) criterion (Adavi et al. 2022):

$$RMSE = \sqrt{\frac{1}{n}\sum_{i=1}^{n}(t_{obs,i} - t_{calc,i})^2} \quad (2)$$

where n denotes the total number of data points, $t_{obs,i}$ is the observed field travel time, and $t_{calc,i}$ represents the travel time calculated from the generated model.

In all models, the RMS error was maintained below 5%, ensuring high reliability of the reconstructed velocity profiles.

RESULTS

The results of the seismic refraction survey, obtained along seven profile lines (RFP-1 to RFP-7), provided detailed insight into the internal structure of the rock mass underlying the tailings facility. By applying the Delta-t-V method, 2D P-wave velocity models were generated, revealing a complex lithological structure characterized by pronounced contrasts between surface embankments, degraded zones, and more compact limestone horizons. The obtained data confirm that the heterogeneity of the rock mass is manifested through abrupt velocity changes, indicating the presence of discontinuities, karstified zones, and degraded rock masses.

In the shallow horizons, to depths of approximately 10–15 m, the recorded velocities range from 600 to 1,200 m/s, corresponding to embankment materials and aeration zones. These values indicate unconsolidated sediments and degraded rocks resulting from mining activities and natural weathering processes. With increasing depth, the velocities progressively increase, reaching values up to 4,400 m/s, which in this study was defined as the seismic threshold for compact limestone units. The boundary of the bedrock is clearly expressed by a sharp increase in velocity, confirming the presence of monolithic horizons with a high degree of consolidation.

To ensure a comprehensive analysis, all seven profile lines (RFP-1 to RFP-7) were interpreted and integrated into the study. The interpretation is performed directly on the cross-sections, where the spatial distribution of key lithological units, including surface embankments, degraded rock masses, and the compact limestone bedrock, is clearly delineated and labeled. The vertical axis was also updated to represent the elevation in meters above sea level [m a.s.l.] to provide a clear scale for the subsurface models. Figures 4–7 show P-wave velocity depth sections along profiles RFP-1 through RFP-4, respectively, where the boundary between the fill material and bedrock is clearly visible. The vertical axis is standardized to represent the elevation in meters above sea level, providing a clear scale for subsurface models. The velocities range from 600 to 1,000 m/s in the near-surface layers, while deeper limestone units reach and exceed 4,400 m/s. This profile is particularly significant as it demonstrates vertical lithological continuity with a clearly defined boundary of the consolidated rock mass at a depth of approximately 35 m.

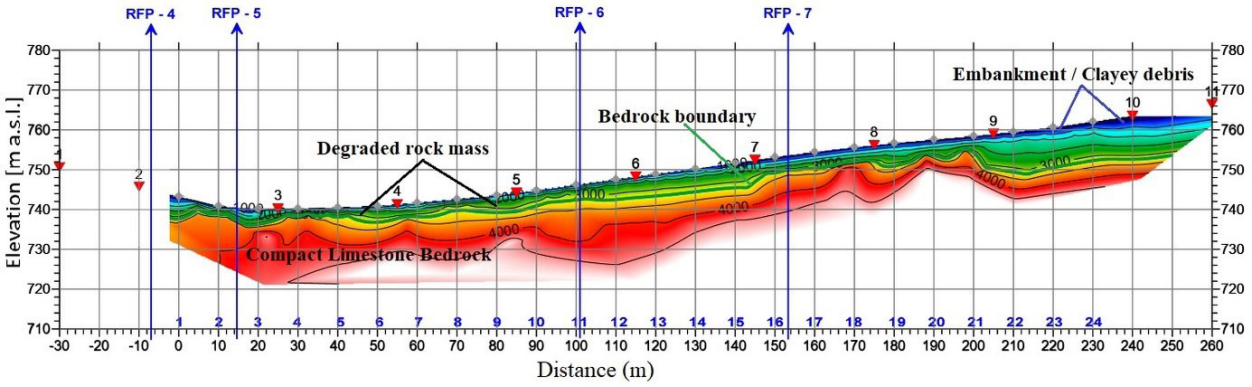

Fig. 4. *2D depth section of P-wave velocities along profile RFP-1. The color scale and contour lines indicate P-wave velocities in meters per second. The vertical axis represents elevation in meters above sea level [m a.s.l.]*

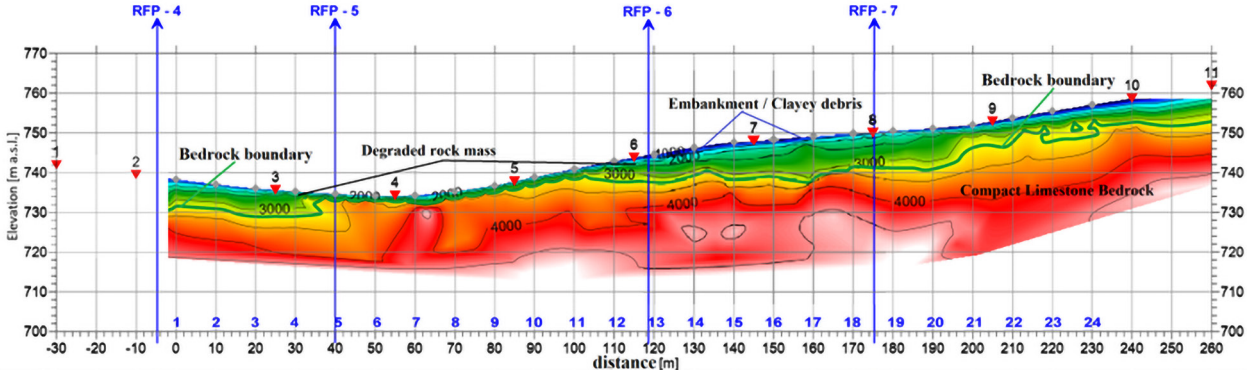

Fig. 5. *2D depth section of P-wave velocities along profile RFP-2. The color scale and contour lines indicate P-wave velocities in meters per second. The vertical axis represents elevation in meters above sea level [m a.s.l.]*

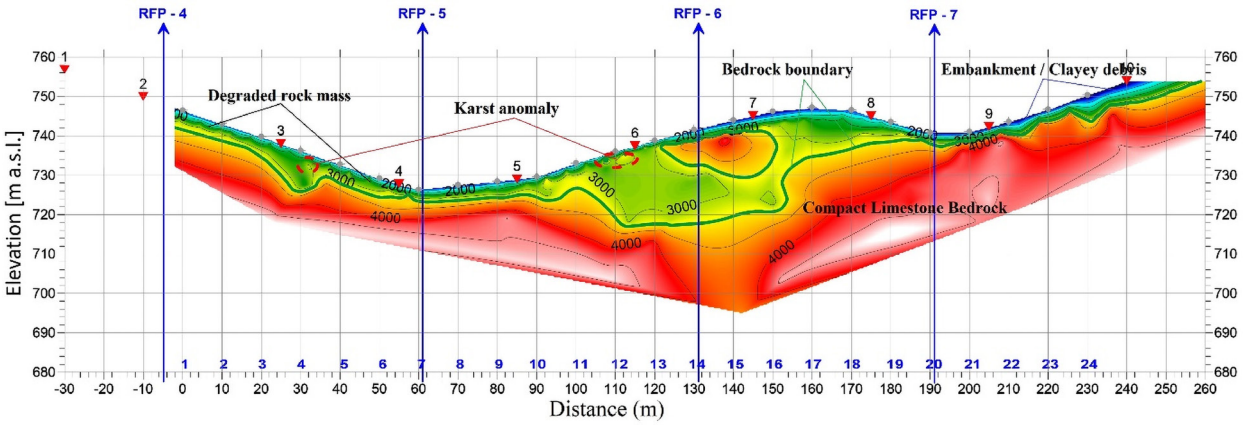

Fig. 6. *2D depth section of P-wave velocities along profile RFP-3. The color scale and contour lines indicate P-wave velocities in meters per second. The vertical axis represents elevation in meters above sea level [m a.s.l.]*

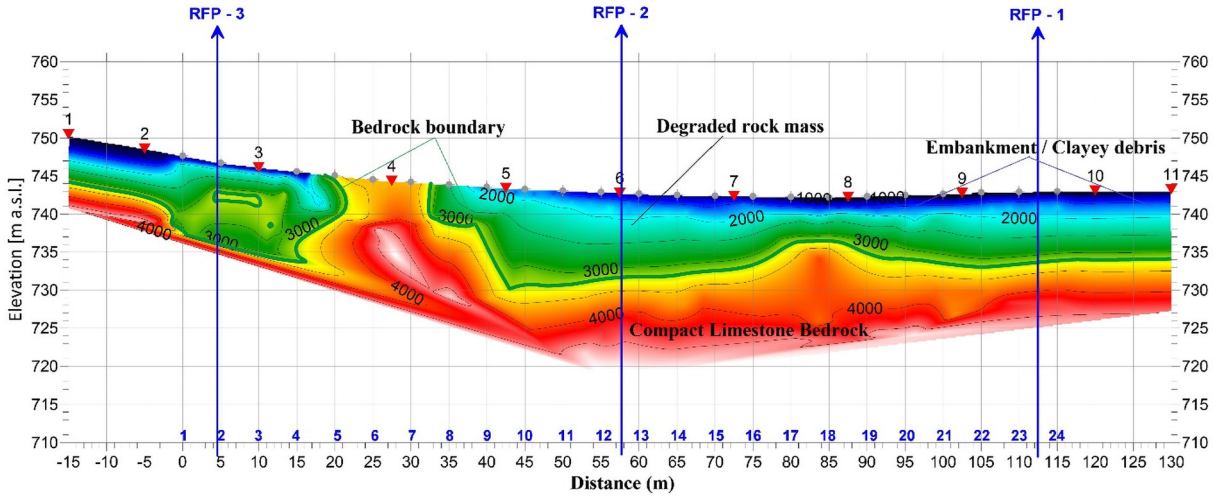

Fig. 7. *2D depth section of P-wave velocities along profile RFP-4. The color scale and contour lines indicate P-wave velocities in meters per second. The vertical axis represents elevation in meters above sea level [m a.s.l.]*

Figures 8–10 present P-wave velocity depth sections along profiles RFP-5, RFP-6, and RFP-7, respectively, where karst structures and degraded zones are clearly identified. Near-surface layers exhibit velocities ranging from 800 to 1,200 m/s, while the compact bedrock in the basal parts exceeds 4,400 m/s. These profiles highlight characteristic anomalies typical of the investigated area, including localized low-velocity zones within deeper horizons. These features are interpreted as cavernous structures and degraded limestone units, indicating spatial variability within the consolidated rock mass.

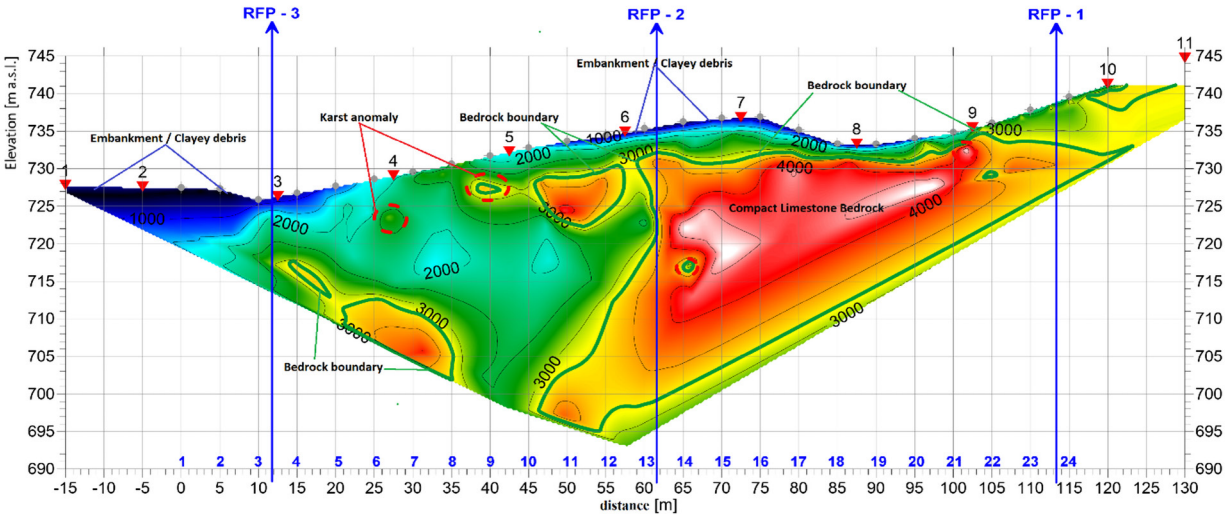

Fig. 8. *2D depth section of P-wave velocities along profile RFP-5. The color scale and contour lines indicate P-wave velocities in meters per second. The vertical axis represents elevation in meters above sea level [m a.s.l.]*

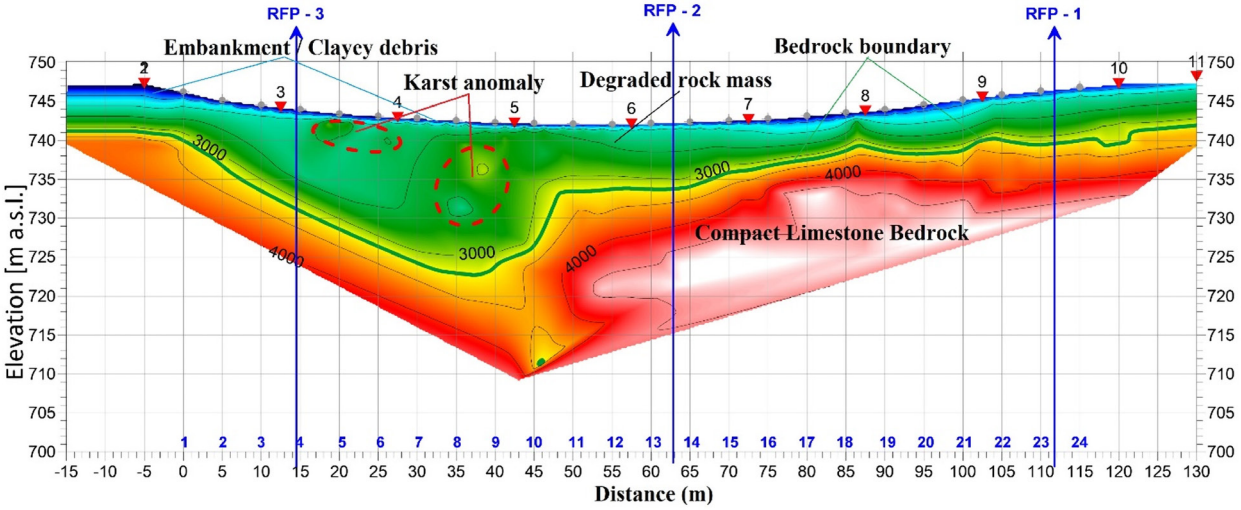

Fig. 9. *2D depth section of P-wave velocities along profile RFP-6. The color scale and contour lines indicate P-wave velocities in meters per second. The vertical axis represents elevation in meters above sea level [m a.s.l.]*

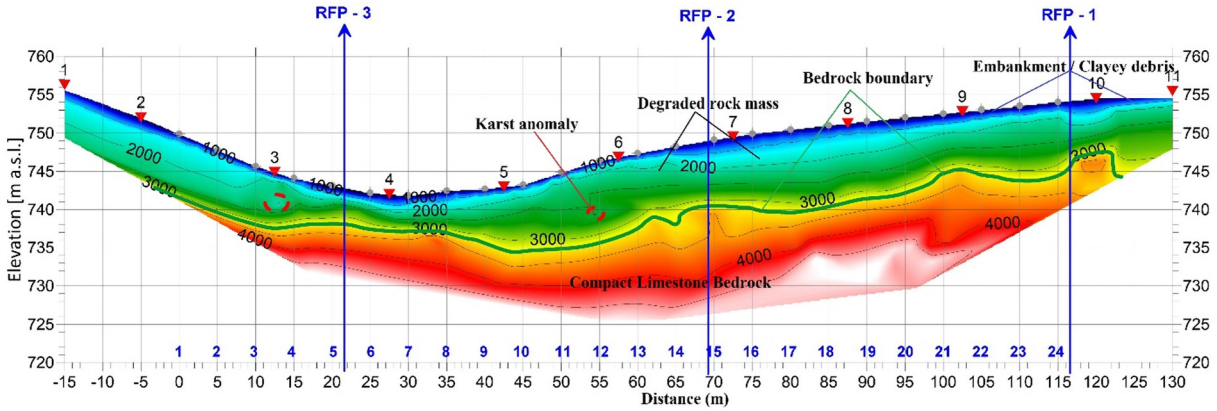

Fig. 10. *2D depth section of P-wave velocities along profile RFP-7. The color scale and contour lines indicate P-wave velocities in meters per second. The vertical axis represents elevation in meters above sea level [m a.s.l.]*

The bedrock boundary consistently manifests as a sharp velocity increase exceeding 4,400 m/s, while shallower horizons are characterized by unconsolidated materials and karstified units. A quasi-3D visualization (fence diagram) of the rock mass was constructed by integrating the individual profiles, providing a comprehensive visualization of the spatial distribution of the lithological units and anomalies (Fig. 11). This spatial representation clearly delineates the bedrock boundary, the distribution of degraded zones, and their relationship to the surface embankments. It confirms the findings obtained from the individual profiles and makes a detailed spatial analysis of the structural discontinuities possible. Figure 11 presents the integrated quasi-3D visualization (fence diagram) of the rock mass within the investigated area.

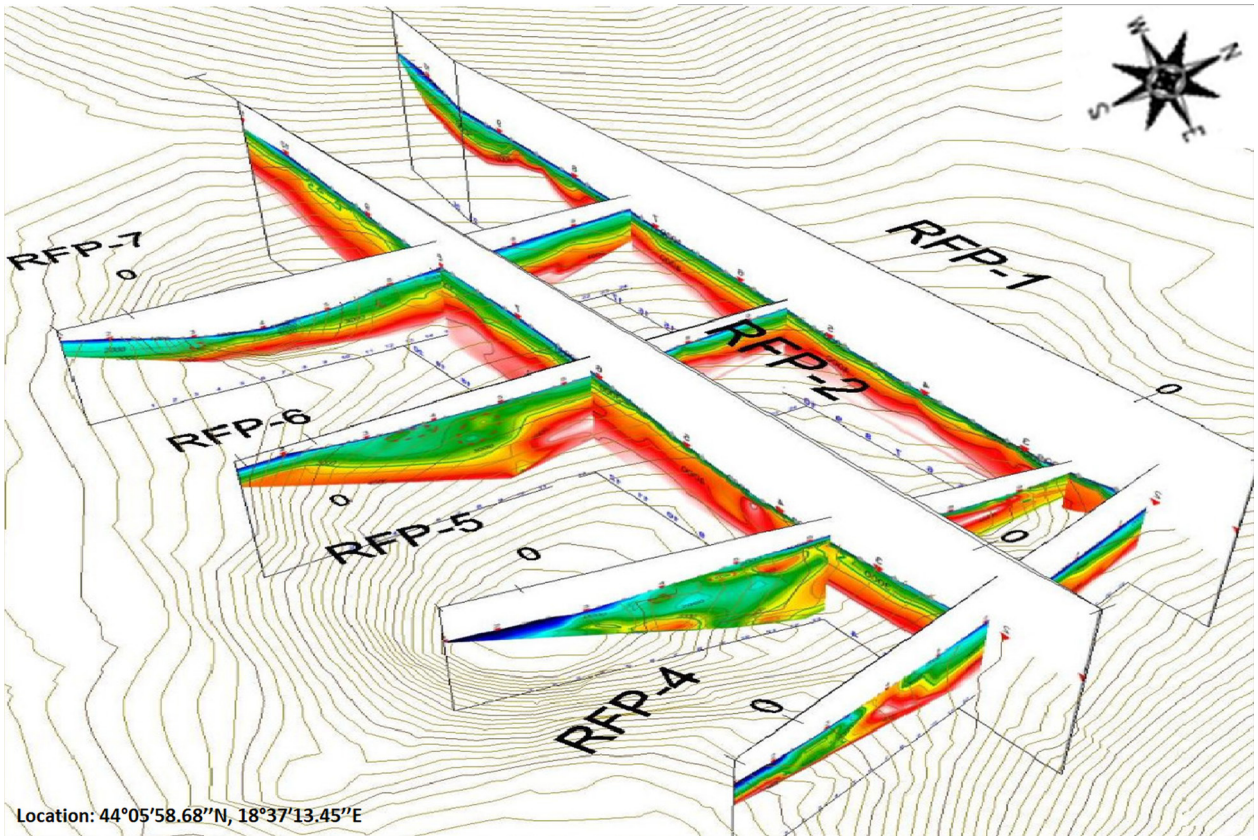

Fig. 11. *Quasi-3D visualization (fence diagram) of P-wave velocity depth sections showing the spatial distribution of lithological units and structural anomalies within the investigated rock mass*

DISCUSSION

The recorded variations in P-wave velocities indicate a direct correlation between the elastic properties of the medium and the degree of tectonic damage and karstification of the terrain (Bektašević et al. 2025d). These results are consistent with previous investigations of damage zones, where seismic methods have shown high reliability in defining the depth and extent of degraded horizons (Bektašević et al. 2024a, 2024b). Analysis of the tomographic models along profiles RFP-1 to RFP-7 enabled precise numerical and lithological classification of the rock mass. P-wave velocities within the shallowest horizons range from 600 to 1,200 m/s, corresponding to unconsolidated surface materials, tailings embankments, and aeration zones, all characterized by high porosity. The intermediate portion of the models is characterized by velocities between 1,800 and 3,200 m/s, indicating a transitional zone of intense karstification. The basal horizon, where velocities reach approximately 4,400 m/s, was identified as the boundary marking the onset of massive and monolithic limestone units. In profile RFP-2, the bedrock boundary is expressed through a sharp vertical velocity gradient, confirming the presence of stable and monolithic horizons at depths greater than 30 m. In contrast, profile RFP-5 exhibits significant local velocity inversions, which represent a clear indicator of karst structures and cavernous zones within the rock mass. Particular attention was given to profile RFP-6 (Fig. 12), where distinctive ring-shaped low-velocity anomalies were identified within zones of relatively high velocities.

To eliminate the possibility of inversion artifacts, the velocity models were cross-validated by ensuring a high ray-tracing density and verifying the stability of the solution across overlapping profile segments.

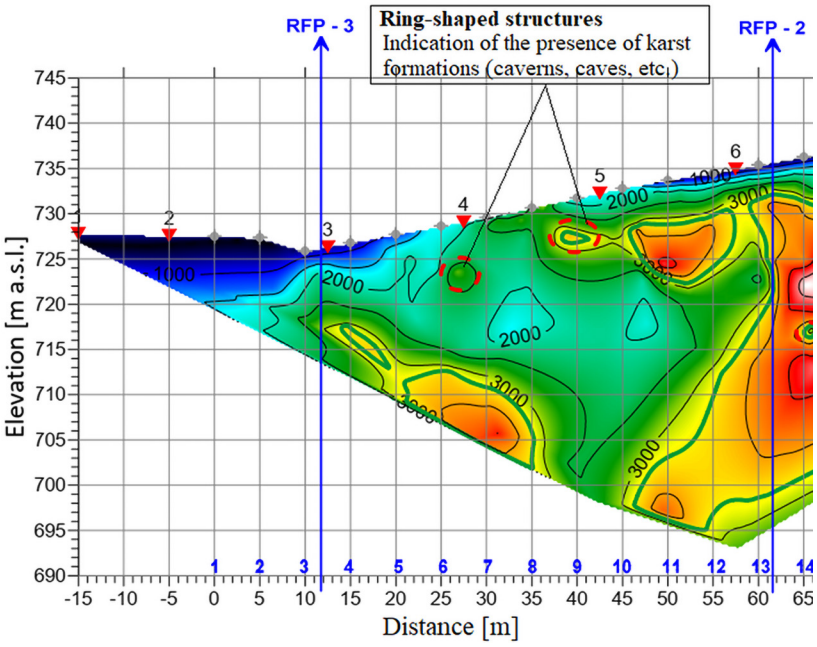

Fig. 12. *2D P-wave velocity model along profile RFP-6. Interpretation highlights localized ring-shaped low-velocity anomalies within the limestone bedrock, interpreted as karst cavities. The vertical axis represents elevation in meters above sea level [m a.s.l.]*

Since the spatial extent of the identified ring-shaped anomalies exceeds the geophone spacing (d_x = 5 m), they are interpreted as physical geological features rather than numerical noise. Furthermore, the sharp velocity contrast (exceeding 2,000 m/s) between these zones and the surrounding bedrock is consistent with the documented karst morphology of this region, which is typically characterized by air- or clay-filled cavities.

Such structures provide direct evidence of developed karst formations, including subsurface cavities and cave systems. Visualization of these results was performed using Delaunay triangulation, ensuring a continuous and accurate representation of the geometry of these subsurface discontinuities – features that conventional refraction methods often fail to resolve adequately.

A lithological classification based on P-wave velocity ranges was developed in order to systematize the interpretation and facilitate practical application of the results, as shown in Figure 13. This classification enables direct correlation between the visual color-coded velocity models and the engineering-geological characteristics of the terrain.

Seismic data obtained through the application of the Delta-t-V method clearly demonstrate pronounced heterogeneity of the rock mass underlying the tailings facility, with well-defined contrasts between surface embankments, degraded zones, and more compact limestone horizons. The recorded variations in P-wave velocities indicate a direct correlation between the elastic properties of the medium and the degree of tectonic damage and karstification of the terrain. These findings are consistent with previous investigations of damage zones, where seismic methods have demonstrated high reliability in defining the depth and extent of degraded horizons. Nevertheless, certain methodological limitations remain. The heterogeneity of near-surface layers and the presence of unconsolidated materials may affect the precision of defining deeper boundaries. Although tomographic models are numerically stable, they are inherently prone to smooth solutions that may obscure localized anomalies. Furthermore, the interpretation of low-velocity zones as karst structures requires caution, as similar velocity values may also result from increased moisture content or technical artifacts.

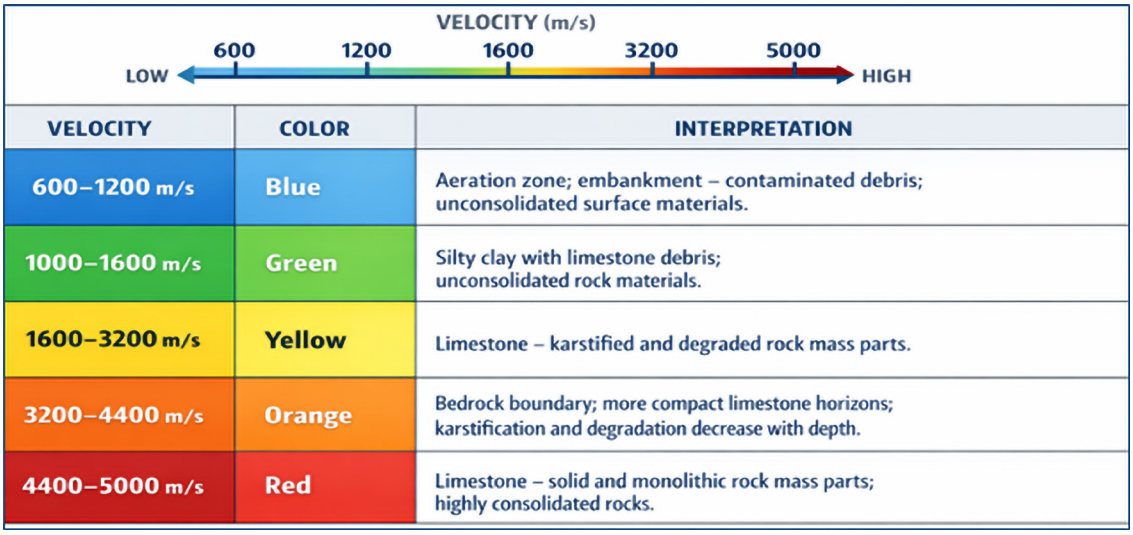

VELOCITY	COLOR	INTERPRETATION
600–1200 m/s	Blue	Aeration zone; embankment – contaminated debris; unconsolidated surface materials.
1000–1600 m/s	Green	Silty clay with limestone debris; unconsolidated rock materials.
1600–3200 m/s	Yellow	Limestone – karstified and degraded rock mass parts.
3200–4400 m/s	Orange	Bedrock boundary; more compact limestone horizons; karstification and degradation decrease with depth.
4400–5000 m/s	Red	Limestone – solid and monolithic rock mass parts; highly consolidated rocks.

Fig. 13. *Lithological identification based on P-wave velocity ranges*

For this reason, the integration of seismic data with invasive geotechnical boreholes and complementary geophysical methods is recommended to validate the findings.

A quasi-3D visualization (fence diagram) was constructed by integrating data from all profiles. This spatial representation enables a comprehensive assessment of the distribution of anomalies, clearly defining the relationship between surface embankments and deeper, stable horizons. Spatial analysis confirms that the most pronounced karst anomalies are concentrated along profiles RFP-3, RFP-5, RFP-6, and RFP-7, suggesting preferential directions of tectonic fracturing followed by subsequent karstification. The application of the Delta-t-V method proved crucial for reliable interpretation under the complex geological conditions of the Olovo mine, as it made it possible to detect the velocity inversions characteristic of karst terrains. However, previous studies indicate that other tomographic algorithms, such as SIRT and Fast Shortest Path, also provide stable results under similar geological conditions. Therefore, the application of the Delta-t-V method in this study should be regarded as a methodological choice adapted to local conditions, rather than as a universally superior technique.

The obtained findings are fully aligned with contemporary trends in geophysical investigations. Brom and Stan-Kłeczek (2015) emphasize the importance of appropriate seismic source selection for optimizing the signal-to-noise ratio in shallow investigations, while Z. Wang et al. (2025) and Bektašević et al. (2025e) highlight the necessity of such multidisciplinary models in the context of quantitative hazard assessment, mining operational safety, and preventive risk management in complex geological environments.

In conclusion, the discussion of the results confirms that seismic tomography provides an objective basis for terrain zoning and stability assessment of tailings facilities, identifying critical zones (cavities) that require enhanced engineering supervision. The obtained findings move beyond general interpretation, providing direct engineering implications for the Olovo mine infrastructure. The identification of localized low-velocity karst anomalies, particularly those highlighted along profile RFP-6, enables precise spatial zoning of the tailings facility. In practical terms, these results dictate the optimization of the geotechnical drilling program, allowing for the strategic placement of boreholes to target identified cavities for subsequent grouting or structural reinforcement. By delineating these critical zones, this study provides a high-resolution foundation for the design of stabilization measures and the implementation of a targeted monitoring regime, significantly mitigating the risk of ground subsidence and ensuring the long-term operational safety of the tailings facility in complex karst environments.

CONCLUSIONS

The conducted seismic refraction investigations at the Olovo tailings facility enabled reliable characterization of the internal structure of the rock mass and delineation of lithological boundaries. The results indicate pronounced heterogeneity of the massif, expressed through contrasts in P-wave velocities between surface embankments and compact limestone horizons.

The basal horizon was clearly identified by a P-wave velocity threshold of approximately 4,400 m/s, marking the transition to monolithic bedrock. The application of the Delta-t-V method, combined with Delaunay triangulation, enabled the detection of ring-shaped anomalies along profiles RFP-3, RFP-5, RFP-6, and RFP-7, indicating karst structures and cavernous zones. Integration of the profiles into a quasi-3D fence diagram confirmed the spatial continuity of weakened zones and highlighted potential directions of structural instability.

Specifically, the identification of localized karst anomalies directly informs the optimization of geotechnical drilling and subsequent grouting programs, allowing for targeted stabilization of the tailings facility.

In future research, the integration of seismic refraction with invasive methods (borehole data and geotechnical sampling) is recommended to further validate the results, along with the implementation of high-resolution spatial seismic tomography for continuous monitoring of structural changes within the tailings facility. Such developments would enhance reliability in stability assessment, making it possible to detect temporal changes in the rock mass state and enable timely response to potential mass instability.

The study confirms that seismic refraction, optimized through appropriate profile geometry and the application of the Delta-t-V method, represents a reliable and interdisciplinary tool for the characterization of complex tailings rock masses. The identification of localized karst anomalies and the definition of the bedrock boundary directly inform the optimization of geotechnical drilling and grouting programs, thereby reducing the uncertainty inherent in subsurface modeling and ensuring the long-term operational safety of the Olovo mine infrastructure. The results provide a high-resolution spatial framework that allows engineers to prioritize intervention zones, significantly lowering the risk of sudden ground subsidence. The obtained results have direct application in mining engineering, engineering geology, and environmental management, while also providing a foundation for further research toward integrated stability assessment methodologies for mining structures. This work therefore constitutes a meaningful contribution to the advancement of mining safety and sustainable tailings management.

Author Luka Crnogorac from the University of Belgrade, Faculty of Mining and Geology would like to express their sincere gratitude for the support provided by the Ministry of Science, Technological Development and Innovation of the Republic of Serbia, within the framework of support for scientific research at the University of Belgrade, Faculty of Mining and Geology in Belgrade, under contract number 451-03-34/2026-03/200126.

REFERENCES

Ackman T.E. & Cohen K.K., 1994. Geophysical methods: Remote techniques applied to mining-related environmental and engineering problems. [in:] *International Land Reclamation and Mine Drainage Conference and Third International Conference on the Abatement of Acidic Drainage. Volume 4: Abandoned Mine Lands and Topical Issues*, United States Department of the Interior, Pittsburgh, PA, 208–217. https://doi.org/10.21000/JASMR94040208.

Adavi Z., Weber R. & Rohm W., 2022. Pre-analysis of GNSS tomography solution using the concept of spread of model resolution matrix. *Journal of Geodesy*, 96(4), 27. https://doi.org/10.1007/s00190-022-01620-1.

Adewoyin O.O., Joshua E.O., Akinyemi M.L., Maxwell O., Aanuoluwa A.T. & Joel E.S., 2021a. Engineering site investigations using surface seismic refraction technique. *IOP Conference Series: Earth and Environmental Science*, 655(1), 012098. https://doi.org/10.1088/1755-1315/655/1/012098.

Adewoyin O.O., Joshua E.O., Akinyemi M.L., Omeje M. & Adagunodo T.A., 2021b. Evaluation of geotechnical parameters of reclaimed land from near-surface seismic refraction method. *Heliyon*, 7(4), e06765. https://doi.org/10.1016/j.heliyon.2021.e06765.

Adewoyin O.O., Joshua E.O., Akinyemi M.L., Omeje M. & Joel E.S., 2021c. Application of seismic refraction in engineering geology. *IOP Conference Series: Earth and Environmental Science*, 655(1), 012102. https://doi.org/10.1088/1755-1315/655/1/012102.

Akingboye A.S., 2025. Electrical and seismic refraction methods: Fundamental concepts, current trends, and emerging machine learning prospects. *Discover Geoscience*, 3(1), 87. https://doi.org/10.1007/s44288-025-00169-8.

Akingboye A.S. & Ogunyele A.C., 2019. Insight into seismic refraction and electrical resistivity tomography techniques in subsurface investigations. *Rudarsko-geološko-naftni zbornik*, 34(1), 93–111. https://doi.org/10.17794/rgn.2019.1.9.

Akinlalu A.A., Futai M.M., Afolabi D.O. & Abraham-A R.M., 2026. A review on the application of geophysical methods in civil engineering studies. *Geosystems and Geoenvironment*, 5(1), 100453. https://doi.org/10.1016/j.geogeo.2025.100453.

Allen C.C., Cracknell M.J., Miller C.B., Missen O.P. & Meffre S., 2025. Practical application of geophysical methods for characterisation of waste rock dumps. *Mine Water and the Environment*. https://doi.org/10.1007/s10230-025-01086-5.

Bačić M., Librić L., Kaćunić D.J. & Kovačević M.S., 2020. The usefulness of seismic surveys for geotechnical engineering in karst: Some practical examples. *Geosciences*, 10(10), 406. https://doi.org/10.3390/geosciences10100406.

Bektašević E., Antičević H., Gutić K. & Sikira D., 2024a. Određivanje dubine zone oštećenja stijenske mase oko profila iskopa miniranjem seizmičkom cross-hole tomografijom u tunelu „Šubir" na autocesti Zagreb–Split [Determination of the depth of the rock mass damage zone around the excavation profile by blasting with seismic cross-hole tomography in the "Šubir" tunnel on the Zagreb–Split motorway]. *Nauka + Praksa*, 27(1), 13–19. https://doi.org/10.62683/NiP27.13-19.

Bektašević E., Antičević H., Gutić K. & Sikira D., 2024b. Application of seismic methods for determining the depth of the rock mass damage zone around the excavation profile by blasting. *Global Journal of Engineering and Technology Advances*, 18(3), 139–151. https://doi.org/10.30574/gjeta.2024.18.3.0051.

Bektašević E., Filipović S., Gutić K. & Musa N., 2025a. Ispitivanje integriteta armiranobetonskih pilota na izlaznom portalu tunela Kobilja Glava nedestruktivnom metodom [Testing the integrity of reinforced concrete piles at the exit portal of the Kobilja Glava tunnel using a non-destructive method]. *e-Zbornik: Electronic Collection of Papers of the Faculty of Civil Engineering*, 15(29), 58–69. https://doi.org/10.47960/2232-9080.2025.29.15.58.

Bektašević E., Filipović S., Hurlov G. & Gutić K., 2025b. Application of a non-destructive method in the analysis of the homogeneity of a concrete foundation in a tunnel structure. *e-Zbornik: Electronic Collection of Papers of the Faculty of Civil Engineering*, 15(30), 71–81. https://doi.org/10.47960/2232-9080.2025.30.15.71.

Bektašević E., Strelec S., Sakić N. & Gutić K., 2025c. Multichannel surface wave analysis in the context of shallow geophysical investigations. *Academia Engineering*, 2(3), 7876. https://doi.org/10.20935/AcadEng7876.

Bektašević E., Mušija A., Gutić K. & Sakić N., 2025d. Application of seismic refraction for determining geomechanical parameters in the excavation zone of the Vranduk tunnel on the Corridor Vc route. [in:] *Proceedings of The International Conference Synergy of Architecture & Civil Engineering, SINARG 2025: Niš (Serbia), September 11–12, 2025*, University, Faculty of Civil Engineering and Architecture, SASA, Branch in Niš, Niš, 513–524. https://doi.org/10.62683/SINARG2025.065.

Bektašević E., Gutić K. & Požegić Z., 2025e. Multidisciplinary analysis of preventive occupational safety measures in tunnel construction. *Journal of Industrial Safety*, 3(1), 59–68. https://doi.org/10.1016/j.jinse.2025.12.002.

Brom A. & Stan-Kłeczek I., 2015. Comparison of seismic sources for shallow seismic: Sledgehammer and pyrotechnics. *Contemporary Trends in Geoscience*, 4(1), 44–53. https://doi.org/10.1515/ctg-2015-0004.

Cai W., Xiang G., Zhang H. & Li Y., 2014. Application of seismic velocity tomography in underground coal mines: A case study of Yima mining area, Henan, China. *Journal of Applied Geophysics*, 109, 140–149. https://doi.org/10.1016/j.jappgeo.2014.07.021.

Cardarelli E., Cercato M., Cerreto A. & Di Filippo G., 2010. Electrical resistivity and seismic refraction tomography to detect buried cavities. *Geophysical Prospecting*, 58(4), 685–695. https://doi.org/10.1111/j.1365-2478.2009.00854.x.

Cheng N., Ismail M.A.B.M. & Nordiana M.M., 2025. From 2D seismic refraction to 3D subsurface characterization: Unpacking the role of univariate spatial interpolation techniques with borehole validation. *Physics and Chemistry of the Earth, Parts A/B/C*, 141, 104113. https://doi.org/10.1016/j.pce.2025.104113.

CTU IPKIN Ltd. Bijeljina, 2022. *Izvještaj rezultata geofizičkih istraživanja u zoni eksploatacijskom polju rudnika olova u Olovu na mikrolokaciji Zone 4 jalovišta u Očeklju*. Centar Tehničkich Usluga IPKIN, Bijeljina [unpublished].

Dean T. & Grant M., 2024. A beginner's guide to seismic sensors. *Australian Society of Exploration Geophysicists*, 230, 38–44. https://doi.org/10.1080/14432471.2024.2395647.

Fisseha S., Mewa G. & Haile T., 2021. Refraction seismic complementing electrical method in subsurface characterization for tunneling in soft pyroclastic: A case study. *Heliyon*, 7(8), e07680. https://doi.org/10.1016/j.heliyon.2021.e07680.

Foti S., Lai C.G., Rix G.J. & Strobbia C., 2018. Guidelines for good practice of surface wave analysis. *Bulletin of Earthquake Engineering*, 16(6), 2367–2420. https://doi.org/10.1007/s10518-017-0206-7.

Gebrande H. & Miller H., 1985. Refraktionsseismik. [in:] *Angewandte Geowissenschaften. Bd. 2: Methoden der angewandten Geophysik und mathematische Verfahren in den Geowissenschaften*, Ferdinand Enke Verlag, Stuttgart, 226–260.

Hanafi L.A., Hardiyatmo H.C. & Faris F., 2025. Liquefaction potential evaluation using near-surface seismic refraction tomography: A case study. *IOP Conference Series: Earth and Environmental Science*, 1458(1), 012036. https://doi.org/10.1088/1755-1315/1458/1/012036.

Herlambang N. & Riyanto A., 2021. Determination of bedrock depth in Universitas Indonesia using the seismic refraction method. *IOP Conference Series: Earth and Environmental Science*, 846(1), 012016. https://doi.org/10.1088/1755-1315/846/1/012016.

Hill J., 2025. *Seismic refraction surveys: An overview of methods and applications*. Douglas Partners. https://www.douglaspartners.com.au/news/seismic-refraction-surveys-an-overview-of-methods-and-applications [access: 3.02.2026].

Idziak A.F. & Dubiel R. (eds.), 2011. *Geophysics in Mining and Environmental Protection*. Springer, Berlin. https://doi.org/10.1007/978-3-642-19097-1.

Jian Z., Zhao G., Ma J., Liu L., Liang W. & Wu S., 2025. Detection of rock mass defects using seismic tomography. *Applied Sciences*, 15(3), 1238. https://doi.org/10.3390/app15031238.

Kalashnikova V., Meisingset I., Øverås R. & Krasova D., 2020. High-resolution seismic velocity field estimation techniques and their application to geohazard, lithology and porosity prediction. *Near Surface Geophysics*, 18(1), 61–72. https://doi.org/10.1002/nsg.12083.

Kuehn T., Holt J.W., Johnson R. & Meng T., 2024. Active seismic refraction, reflection, and surface wave surveys in thick debris covered glacial environments. *Journal of Geophysical Research: Earth Surface*, 129(1), e2023JF007304. https://doi.org/10.1029/2023JF007304.

Lottermoser B.G., 2010. Mine water. [in:] Lottermoser B.G., *Mine Wastes: Characterization, Treatment and Environmental Impacts*, Springer, Berlin, Heidelberg, 119–203. https://doi.org/10.1007/978-3-642-12419-8.

Maniscalco R., Fazio E., Punturo R., Cirrincione R., Di Stefano A., Distefano S., Forzese M., Lanzafame G., Leonardi G.S., Montalbano S., Pellegrino A.G., Raele A. & Palmeri G., 2022. The porosity in heterogeneous carbonate reservoir rocks: Tectonic versus diagenetic imprint – A multi-scale study from the Hyblean Plateau (SE Sicily, Italy). *Geosciences*, 12(4), 149. https://doi.org/10.3390/geosciences12040149.

Mollehuara-Canales R., Lghoul M., Kchikach A., Hakkou R. & Guerin R., 2021. Leveraging active-source seismic data in mining tailings: refraction and MASW analysis, elastic parameters, and hydrogeological. *Bulletin of the Geological Society of Finland*, 93(2), 105–127. https://doi.org/10.17741/bgsf/93.2.002.

Musmann P., 2023. Determination of seismic resolution: Some practical aspects from land seismic data. [in:] *GeoBerlin 2023*. https://doi.org/10.48380/h6nm-zc18.

Padovan B., Bačić M., Librić L., Mejrušić V. & Kovačević M.S., 2025. Multi-geophysical characterization of karst landfills in Croatia: Mapping the waste–bedrock interface and assessing waste volume. *Sustainability*, 17(24), 10892. https://doi.org/10.3390/su172410892.

Pegah E. & Liu H., 2016. Application of near surface seismic refraction tomography and multichannel analysis of surface waves for geotechnical site characterizations: A case study. *Engineering Geology*, 208, 100–113. https://doi.org/10.1016/j.enggeo.2016.04.021.

Sandmeier K.J., 2016. *ReflexW version 8.1: Program for processing of seismic, acoustic or electromagnetic reflection, refraction and transmission data* [software manual]. Sandmeier Software, Karlsruhe, Germany.

Sheehan J.R., Doll W.E., Watson D.B. & Mandell W.A., 2005. Application of seismic refraction tomography to karst cavities. [in:] *U.S. Geological Survey Karst Interest Group Proceedings, Rapid City, South Dakota, September 12–15, 2005*, Scientific Investigations Report 2005-5160, U.S. Department of the Interior, U.S. Geological Survey, 29–38. https://pubs.usgs.gov/sir/2005/5160/PDF/Part1_2.pdf.

Sheriff R.E. & Geldart L.P., 1995. *Exploration Seismology* (2nd ed.). Cambridge University Press, Cambridge. https://doi.org/10.1017/CBO9781139167932.

Steeples D.W., 2005. Shallow seismic methods. [in:] Rubin Y. & Hubbard S.S. (eds.), *Hydrogeophysics*, Water Science and Technology Library, 50, Springer, Dordrecht, 215–251. https://doi.org/10.1007/1-4020-3102-5_8.

Sun L., Zhou H.-W., Zou Z., Hu H., Wo Y. & Ding Y., 2025. Quantifiable elements of seismic image fidelity: A tutorial review. *Geosciences*, 15(12), 445. https://doi.org/10.3390/geosciences15120445.

Tajudin S.A.A., Abidin M.H.Z., Madun A. & Zawawi M.H., 2016. Barren acidic soil assessment using seismic refraction survey. *IOP Conference Series: Materials Science and Engineering*, 136(1), 012035. https://doi.org/10.1088/1757-899X/136/1/012035.

U.S. EPA, 2026. *Seismic Refraction*. U.S. Environmental Protection Agency. https://www.epa.gov/environmental-geophysics/seismic-refraction [access: 3.02.2026].

Vick S.G., 1990. *Planning, Design, and Analysis of Tailings Dams*. BiTech Publishers, Richmond.

Wang H., Wang J., Yin X. & Liang X., 2025. Quantitative hazard assessment of mining-induced seismicity using spatiotemporal *b*-value dynamics from microseismic monitoring. *Applied Sciences*, 15(18), 10073. https://doi.org/10.3390/app151810073.

Wang Z., Juhlin C., Lü Q., Ruan X., Liu Z., Yu C. & Chen M., 2025. High-resolution seismic reflection surveying to delineate shallow subsurface geological structures in the karst area of Shenzhen, China. *Solid Earth*, 16(3), 761–773. https://doi.org/10.5194/se-16-761-2025.

Watts H., Booth A.D., Reinardy B.T.I., Killingbeck S.F., Jansson P., Clark R.A., Chandler B.M.P. & Nesje A., 2022. An assessment of geophysical survey techniques for characterising the subsurface around glacier margins, and recommendations for future applications. *Frontiers in Earth Science*, 10, 734682. https://doi.org/10.3389/feart.2022.734682.

Wei W. & Fu L.-Y., 2014. On horizontal resolution for seismic acquisition geometries in complex 3D media. *Journal of Applied Geophysics*, 108, 43–52. https://doi.org/10.1016/j.jappgeo.2014.06.011.

Xie L., Wang B., Wang Y., Fang J., Zeng L., Xin G., Shen S. & She Z., 2024. The method for precise seismic detection of geological structures in underground coal mines and application. *Frontiers in Earth Science*, 12, 1307275. https://doi.org/10.3389/feart.2024.1307275.

Yilmaz Ö., 2001. *Seismic Data Analysis: Processing, Inversion, and Interpretation of Seismic Data* (2nd ed.). Society of Exploration Geophysicists, Tulsa. https://doi.org/10.1190/1.9781560801580.